高 分 子 学 报
ACTA POLYMERICA SINICA

综述
Review

DOI: 10.11777/j.issn1000-3304.2026.26251
CSTR: 32057.14.GFZXB.2026.7721

聚乳酸熔融沉积3D打印件的层间界面增强研究进展

高 霞[1*] 黄诚祥[1] 孙得翔[1] 苏允兰[2*] 陈 锐[3]

([1]西南交通大学化学学院 成都 610031)
([2]中国科学院化学研究所 北京 100190)
([3]深圳光华伟业股份有限公司 武汉 430200)

摘 要 作为熔融沉积成型(fused deposition modeling，FDM)技术应用最广泛的3D打印材料之一，聚乳酸(poly(lactic acid)，PLA)具有可再生、可降解、挤出流动性好、成型温度低和尺寸精度高等诸多优点. 然而，由于常压下逐层堆积的成型工艺，PLA打印件普遍存在结晶度低、层间结合不充分等问题，导致其力学性能低于传统注塑件、且呈现显著力学各向异性，严重制约了其作为承载结构件和功能部件的应用. 本综述从PLA材料本征特性与FDM成型工艺的匹配性出发，系统分析了PLA在熔融挤出、熔体沉积及冷却固化等关键阶段中的熔体流变行为、结晶特性及分子链互扩散与缠结行为，全面分析了PLA优异可打印性的内在机理. 进而，针对PLA层间结合薄弱问题，系统综述了近年来围绕层间界面增强所开展的系列研究，重点分析材料改性、打印工艺、外场辅助及后处理等增强策略对层间界面结构与性能的影响机制. 最后，展望了聚乳酸3D打印的未来发展方向，为高性能、智能化PLA材料与制件的设计提供参考.

关键词 熔融沉积成型；聚乳酸材料；可打印性；层间界面增强

Recent Advances of Enhancing Interlayer Bonding of Poly(lactic acid) Materials Fabricated by Fused Deposition Modeling

Xia Gao[1*], Cheng-xiang Huang[1], De-xiang Sun[1], Yun-lan Su[2*], Rui Chen[3]

([1]*School of chemistry, Southwest Jiaotong University, Chengdu 610031*)
([2]*Institute of Chemistry Chinese Academy of Sciences, Beijing 100190*)
([3]*Shenzhen Esun Industrial Co., Ltd., Wuhan 430200*)

Abstract As one of the most widely accepted printing materials for fused deposition modeling (FDM) technique, poly(lactic acid) (PLA) offers numerous advantages, including renewability, biodegradability, excellent flowability, low printing temperature, and high dimensional accuracy. However, due to the layer-by-layer process intrinsic for FDM process, 3D-printed PLA parts tend to suffer from low crystallinity and poor interlayer bond quality, resulting in inferior and anisotropic mechanical properties compared to those of conventional injection-molded parts, which severely restricts their applications as load-bearing structural components and functional parts. This review, for the first time, focused on the adaptability of PLA materials to the FDM process from the material perspective, systematically analyzed their rheological behavior, crystallization characteristics, and molecular chain interdiffusion and entanglement of PLA during the key FDM sub-processes, including material extrusion, melt deposition, and interlayer bonding. In this regard, the excellent printability of PLA materials was thoroughly elucidated. Then, to address the interlayer bonding issue in PLA printing, this review presented a comprehensive overview of recent studies on bond interface enhancement, categorizing the main strategies into material modification, printing process optimization, external-field assistance and post-treatment, and discussing

Received 2026-07-23, Accepted 2026-08-24, Published online .
* Corresponding author, E-mail: gaoxia@swjtu.edu.cn; ylsu@iccas.ac.cn

their effects on interfacial microstructure and mechanical properties. Finally, we presented an outlook on future developments for PLA printing, providing a reference for the design of PLA materials and their components with excellent performances and functionality.

Keywords Fused deposition modeling; Poly(lactic acid); Printability; Interfacial bonding enhancement

引用: 高霞, 黄诚祥, 孙得翔, 苏允兰, 陈锐. 聚乳酸熔融沉积3D打印件的层间界面增强研究进展. 高分子学报, doi: 10.11777/j.issn1000-3304.2026.26251.

Citation: Gao, X.; Huang, C. X.; Sun, D. X.; Su, Y. L.; Chen, R. Recent advances of enhancing interlayer bonding of poly(lactic acid) materials fabricated by fused deposition modeling. *Acta Polymerica Sinica* (in Chinese), doi: 10.11777/j.issn1000-3304.2026.26251.

熔融沉积成型(fused deposition modeling，FDM)，亦称熔丝制造(fused filament fabrication，FFF)，是材料挤出式增材制造技术(3D打印技术)最具代表性的工艺. 该工艺通过带液化器的喷嘴将热塑性聚合物材料熔融挤出，并按照预定路径逐层沉积，从而制造三维物理实体[1,2]. 与其他聚合物3D打印工艺相比，FDM技术的材料适用范围广，设备维护成本低，工艺能耗少，工作环境友好[3]. 更重要的是，FDM工艺灵活性高，可支持多喷头协同工作，同步打印多种材料，显著提高制件的结构复杂性及功能多样性[4~6]. FDM设备还可配备活塞式或螺杆式挤出系统，并采用大尺寸喷嘴设计，直接以聚合物颗粒为原料，克服传统丝材喂料与挤出系统在材料种类、成型空间和成型速度方面的限制，实现大型构件的高速制造[7]. 据报道，Cincinnati公司的BAAM打印机(big-area additive manufacturing，大面积增材制造)成型体积可达10.7~25.5 m^3，熔体流速最高为45 kg/h[1,7]. FDM技术还可与形状记忆聚合物结合，通过精心设计形变机制、精准调控外部环境，实现静态单功能结构向动态多功能系统的转变，赋予复杂构件环境刺激响应性和功能可定制性，在4D打印领域展现出独特优势[8~10]. 凭借突出的工艺灵活性与成本效益优势，FDM技术已成为目前应用最广泛的3D打印技术，自2011年起占据了行业主导地位，在消费级3D打印市场中的份额超过60%，其应用范围正逐步从快速模型制造向生物医药、仿生机器人、汽车制造等高端领域延伸[11,12].

聚乳酸(poly(lactic acid)，PLA)是一种热塑性聚合物，由玉米、甘蔗等生物质原料发酵而成的乳酸单体直接缩聚合成，或由环状丙交酯开环聚合而成[13]，是现阶段FDM工艺应用最多的打印材料之一，其市场占有率达40%. 作为3D打印材料，PLA具有熔融流动性好、尺寸精度高、无明显毒性和气味、来源可再生、可生物降解、可形状记忆等优点[14,15]，广泛应用于模型、医疗辅助器械、组织工程、智能响应等领域的产品设计与开发[16,17]. 然而，受材料本身结晶能力弱、FDM成型热历史复杂的影响，聚乳酸3D打印件普遍存在层间结合薄弱、力学各向异性显著、脆性大、耐热差等问题，制约着聚乳酸3D打印材料的发展、3D打印制品的应用及FDM技术潜能的充分发挥，亟待通过理论研究、材料创新、工艺升级来实现材料与技术突破. 基于此，本综述从PLA本征特性与FDM打印工艺的匹配性出发，梳理了PLA材料的3D打印性，并重点聚焦其层间结合薄弱这一关键问题，评述了近年来围绕层间界面结构与性能调控的研究进展，期望为聚乳酸3D打印材料开发、聚乳酸3D打印件增强及其应用推广提供理论参考.

1 聚乳酸材料的3D打印性

FDM技术通过热塑性高分子的熔融挤出与层层堆积冷却实现成型，其工艺特性要求打印材料兼具优异的可挤出性、良好的尺寸稳定性及足够的结构支撑性等[18,19]. 与其他热塑性聚合物相比，PLA材料展现出非常优异的3D打印性能，这与其力学性能、流变行为及结晶特性密不可分[20~22]. 本部分从PLA本体的结构与性能出发，结合其在FDM挤出、沉积与固化等阶段的成型特点，分析其优良3D打印特性的内在机理.

1.1 聚乳酸的可挤出性

FDM成型的第一步是材料熔融挤出，这要求3D打印材料具有良好的可挤出性，即熔融或半熔融的聚合物材料能在挤出系统提供的压力限值内，以稳定的体积流速(Q)流经直径小于1 mm的喷嘴，形成连续均匀的细丝(图1a). 在通用打印温度和打印速率下，聚合物熔体在流经长度为L、直径为R的喷嘴时所承受的剪切速率高达100~1000 s^{-1}，并产生约20~35 MPa压力降ΔP (公式1)[23].

$$\Delta P = \frac{8\eta QL}{\pi R^4} \quad (1)$$

由公式(1)可知，适用于FDM工艺的热塑性聚合物应具有较低的剪切黏度(η)，以降低熔体流经喷嘴时的压力降，从而保障熔体顺利挤出. 此外，该类材料还应呈现剪切变稀的流变特性，使其熔体在喷嘴内黏度因剪切作用而显著降低，实现低压力稳定挤出；而在离开喷嘴后，黏度迅速恢复至零切条件下的高黏度状态，确保挤出物的几何结构稳定性[18,24,25]. 反之，若聚合物熔体表现为剪切增稠，则挤出过程中黏度随剪切速率升高而增大，易导致喷嘴阻塞.

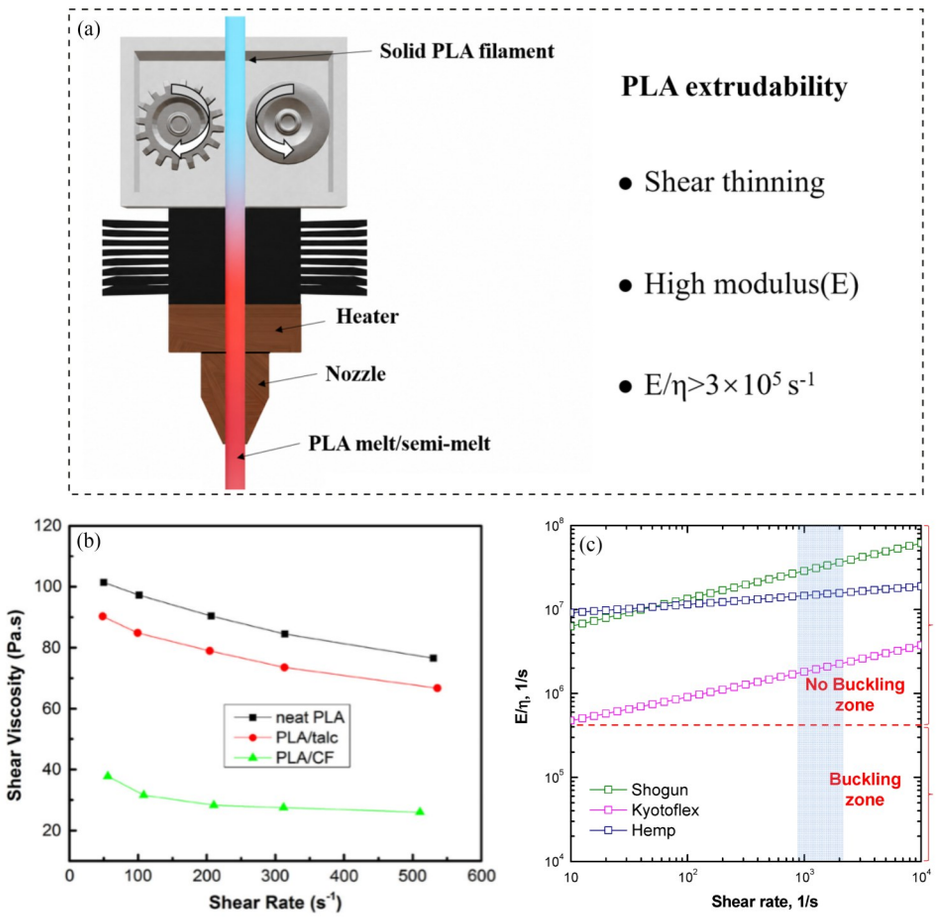


Fig. 1 Extrudability of PLA materials during FDM process: (a) schematic illustration of PLA melt extrusion through a nozzle; (b) apparent viscosities of various PLA-based filaments. The test temperature was 230 ℃, the same as the nozzle temperature during FDM process (Reprinted with permission from Ref. [27]; Copyright (2019) John Wiley & Sons, Inc); (c) buckling analysis performed on PLA-based materials (Reproduced from Ref. [29]; Copyright (2022) The Author(s), under the terms of the Creative Commons Attribution 4.0 International License (CC BY 4.0)).

PLA及其复合材料的熔体属于典型非牛顿流体，其动态流变行为呈现以下特征：在低频区的复数黏度对频率变化不敏感，呈现牛顿平台，其值约为10^3~10^5 Pa·s；随着频率增加至10 rad/s以上，分子链逐渐沿流动方向取向并解缠结，导致熔体黏度下降，表现出剪切变稀行为[26]. 在FDM剪切速率范围内，PLA黏度降低至200~400 Pa·s (图1b)[27]，所产生的ΔP远小于10 MPa[28]，这使其仅需较小的挤出压力并稳定流出，而后又迅速恢复较高黏度，保持打印结构的尺寸稳定性. 换言之，PLA材料可在FDM挤出系统提供的压力限值内，实现快速打印[29].

PLA的挤出性还与其力学性能密切相关. 在FDM成型中，直径为1.75 mm的丝材经夹送辊推送进入喷嘴，未熔融的丝材段充当活塞，挤压喷嘴内熔融/半熔融物料，以实现熔体挤出. 若固态丝材的刚度不足以抵抗喷嘴内熔体流动所需的压力，线材将发生屈服失稳现象，导致挤出失败[30]. 学者们将材料的欧拉临界屈服应力(σ_{cr})与熔体挤出压力降(ΔP)相关联，发现当材料的弹性模量(E)与剪切黏度(η)之比低于临界值(3×10^5~5×10^5 s^{-1})时，丝材屈曲发生[31,32]. PLA是一种刚性聚合物，其本体强度和

模量可与聚对苯二甲酸乙二醇酯(PET)的相媲美[17,22]. 例如，聚左旋乳酸(poly(L-lactide)，PLLA)或聚右旋乳酸(poly(D-lactide)，PDLA)呈半结晶性，其拉伸强度为45~70 MPa，弹性模量为3~4 GPa[17,33]. 当被制成直径为1.75 mm的3D打印线材，PLA材料的拉伸强度和模量与本体的相当[10]. Arrigo等[29]计算了多种PLA打印材料在FDM剪切速率范围内的E/η值，发现其均位于无屈曲安全区(图1c). 总之，PLA凭借其优异的力学性能、剪切变稀的熔体特性，在FDM挤出阶段表现出优异的可挤出性.

1.2 聚乳酸的打印精度

FDM成型的第二步为熔体沉积，将离开喷嘴的熔体以细丝形式按照预定路径沉积在基板表面. 熔体离开喷嘴后，因剪切力被移除而应力松弛，易发生挤出胀大(图2a)，影响3D打印件的成型精

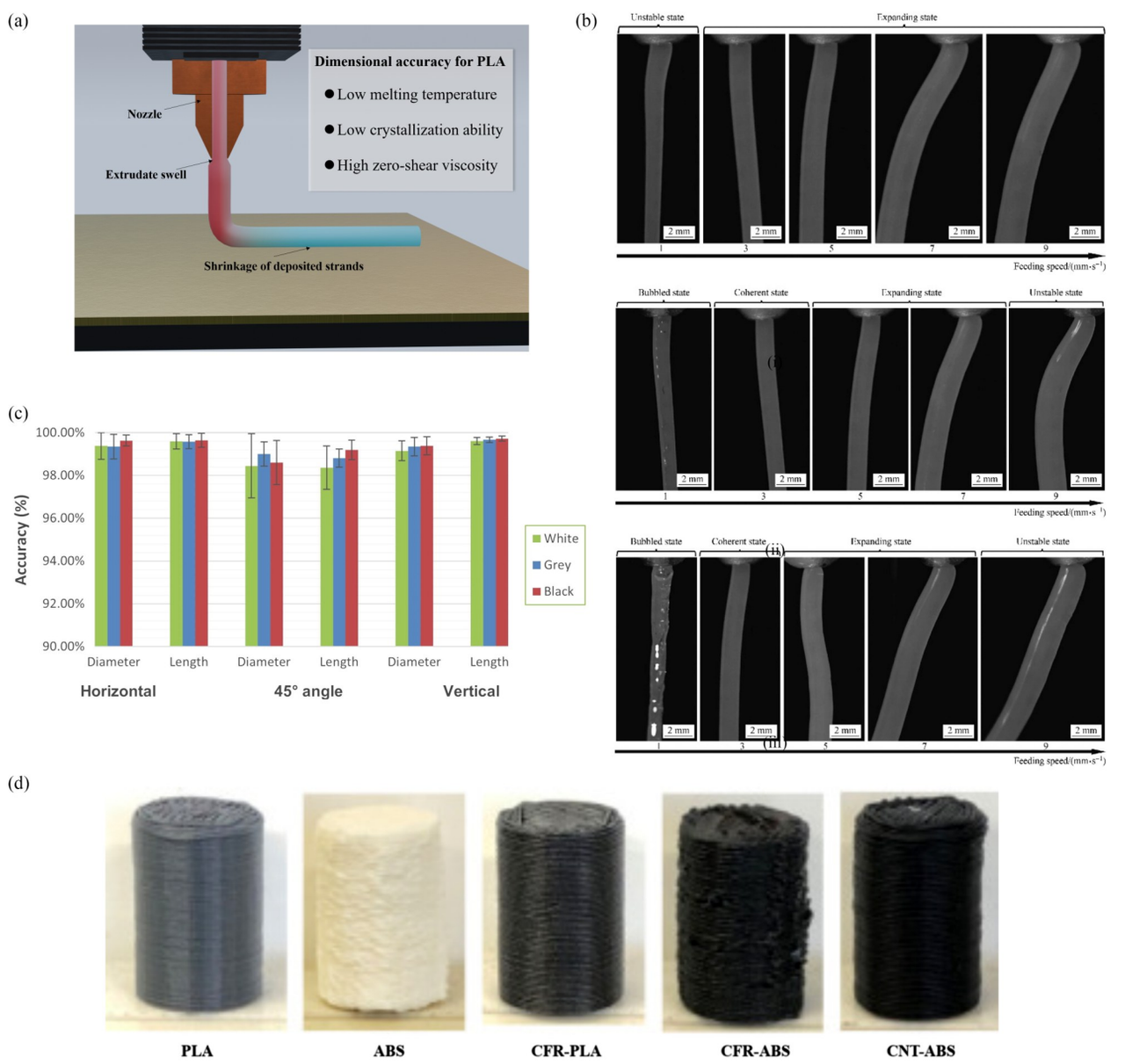


Fig. 2 Dimensional accuracy of FDM-printed PLA samples: (a) schematic illustration of geometrical change in PLA extrudate after extrusion; (b) exit morphology under different feeding speeds at heated block length of 60 mm, printing temperatures of (i) 190 ℃, (ii) 210 ℃, (iii) 230 ℃ (Reprinted with permission from Ref. [39]; Copyright (2023) Springer Nature). (c) The average dimensional (diameter and length) accuracy of cylindrical test specimens manufactured in different print orientations and colors (Reproduced from Ref. [57]; Copyright (2021) Elsevier Ltd., under the terms of the Creative Commons CC BY 4.0). (d) Appearance of printed specimens from PLA, ABS, carbon-fiber-reinforced PLA (CFR-PLA), carbon-fiber-reinforced ABS (CFR-ABS), and CNT-ABS (Reproduced from Ref. [56]; Copyright (2020) The Author(s), under the terms of the Creative Commons Attribution 4.0 International License (CC-BY-NC-ND)).

度[34]. 材料的挤出胀大行为受到材料本身分子量、打印速率及喷嘴直径等因素的影响[35,36]. Tang等[37,38]发现分子量不同的PLA材料在FDM挤出后的胀大行为存在差异. 其中，分子量分布最宽的PLA胀大率最高，这是高分子量组分的高弹性和低分子量组分的延迟链恢复共同叠加的结果. FDM喷嘴内的剪切速率也会影响挤出物的形貌. 当熔体承受的剪切速率低于4000 s^{-1}时，挤出物为表面光滑且规整的圆柱形；当剪切速率达到或超过该临界值时，挤出物因流动失稳而出现“鲨鱼皮”效应(图2b)，降低了PLA打印件的尺寸精度[39]. 在实际PLA打印中，为兼顾挤出稳定性与制件精度，常选用直径为0.4 mm的喷嘴，并控制喷嘴温度小于210 ℃、进料速率低于30 mm/s[40]. 刚沉积于基板表面的PLA熔体仍保有一定流动性，会改变沉积线条的几何形状，进而影响3D打印件的尺寸精度. 研究表明，当PLA材料在低频区域具有显著屈服行为时，其熔体被沉积到底板后因剪切应力被移除而转变为高黏度的类固态，有效抵抗了熔体流动和铺展，可得到较高精度的3D打印件[24,25]. 反之，无屈服应力的PLA材料在沉积后，因零切黏度不会增加而流动，不利于挤出线条的形状稳定性及3D打印件的尺寸精度[29,41].

通常，沉积在底板的PLA线条须快速固化，以稳定挤出线迹的几何形状，为后续层堆积提供基底，保障3D打印件的结构精度与稳定性. 在FDM成型中，聚合物熔体大多在敞开环境下快速冷却，通过结晶或玻璃化转变而固化. 半结晶性聚合物在快速降温时不仅发生大分子链间自由体积和振动体积的减小，还形成致密晶体结构，产生比无定型聚合物更显著的体积收缩和更大的残余内应力，导致3D打印件收缩、翘曲变形，甚至打印失败[42,43]. 因此，适用于FDM技术的材料大多为非晶态高分子，如丙烯腈-丁二烯-苯乙烯共聚物(ABS)、聚碳酸酯(PC)，及熔点低于200 ℃的半结晶聚合物[21]. PLA的玻璃化转变温度(T_g)约在55~65 ℃之间，熔融温度(T_m)在150~180 ℃范围，不仅降低了打印能耗，也减少了热应力对成型件精度的影响[44~46]. 此外，半刚性分子结构限制了PLA分子链的运动与旋转[47]，导致其热收缩率仅为0.2%，远小于ABS (0.6%)、PET (0.3%)[48,49]. 此外，纯PLA的结晶速率较低，其半结晶时间受结晶温度、立体构型及分子量的影响，约为17~45 min，比相同过冷度下等规聚丙烯的半结晶时间大一个数量级[50,51]. 因此，将重均分子量大于200 kg/mol的PLLA熔体以10 ℃/min的速率冷却，即可获得无定形结构[51~53]. 由于FDM成型中降温速率高达100 ℃/s[54]，PLA打印件的结晶度常低于10%，甚至为无定形态[51]；只有借助增塑剂、成核剂，或提高底板温度、延长打印时间等策略，才能将PLA打印件的结晶度提高至30~40%[53,55]. 因此，PLA材料在FDM固化阶段产生的体积收缩较小，其成型件的实际尺寸与模型标称值偏差可控制在2%以内(图2c)[56]，并随着无机填料的加入而进一步提升[27,57~59]，满足高精度FDM成型的要求.

总之，PLA凭借特有的熔体黏弹性及低结晶能力，在熔体沉积及固化过程中表现出优异的成型精度. 在相同打印工艺与表面处理条件下，PLA打印件表面粗糙度始终低于200 μinch (图2d)，显著优于ABS、PET 2种材料所制备的零件[60].

1.3 聚乳酸的层间结合能力

在FDM层层堆积过程中，相邻聚合物细丝通过表面接触、黏性烧结以及分子链跨层扩散与缠结等形成结合界面(图3a)，以保障三维结构的几何与机械稳定性[24,61]. 在此阶段，材料的层间结合能力是决定3D打印件宏观性能的关键. 对于半结晶性聚合物而言，结晶的发生使层间结合较为复杂[15]. 一方面，结晶会显著提高熔体黏度，抑制黏性烧结颈的生长，阻碍界面分子链的互扩散；另一方面，在界面处形成的晶体能够通过物理“锚定”作用强化相邻薄层中分子链的缠结网络. 由此，3D打印件的层间结合性能最终由结晶与分子链扩散相互竞争而形成的界面微观结构所决定[62,63]. 由于PLA的结晶速率相对较慢，大部分3D打印件的结晶度低于5%，其结晶对界面处的黏性烧结与分子链互扩散的影响较小或可被忽略. 大多情况下，PLA的层间结合机理与无定形聚合物的相似，主要由熔体黏度和分子链运动能力决定. Shmueli等[64]发现，通过控制喷嘴温度在215~245 ℃范围内，PLA在水平与垂直方向的界面互扩散长度就可接近分子链的均方旋转半径(R_g)，实现充分的层间结合.

综上，PLA具有优异的可挤出性、良好的成型尺寸精度及一定的层间结合能力，能够适配FDM成型的所有工艺要求，因而成为目前应用最广泛的3D打印材料之一.

然而，FDM成型在常温常压下进行，打印材料的温度常以约100 ℃/s降至T_g以下，导致层间有效结合时间不足1 s[52]，这使得大多PLA打印件内部存在大量介孔，且层间界面的分子链缠结网络密

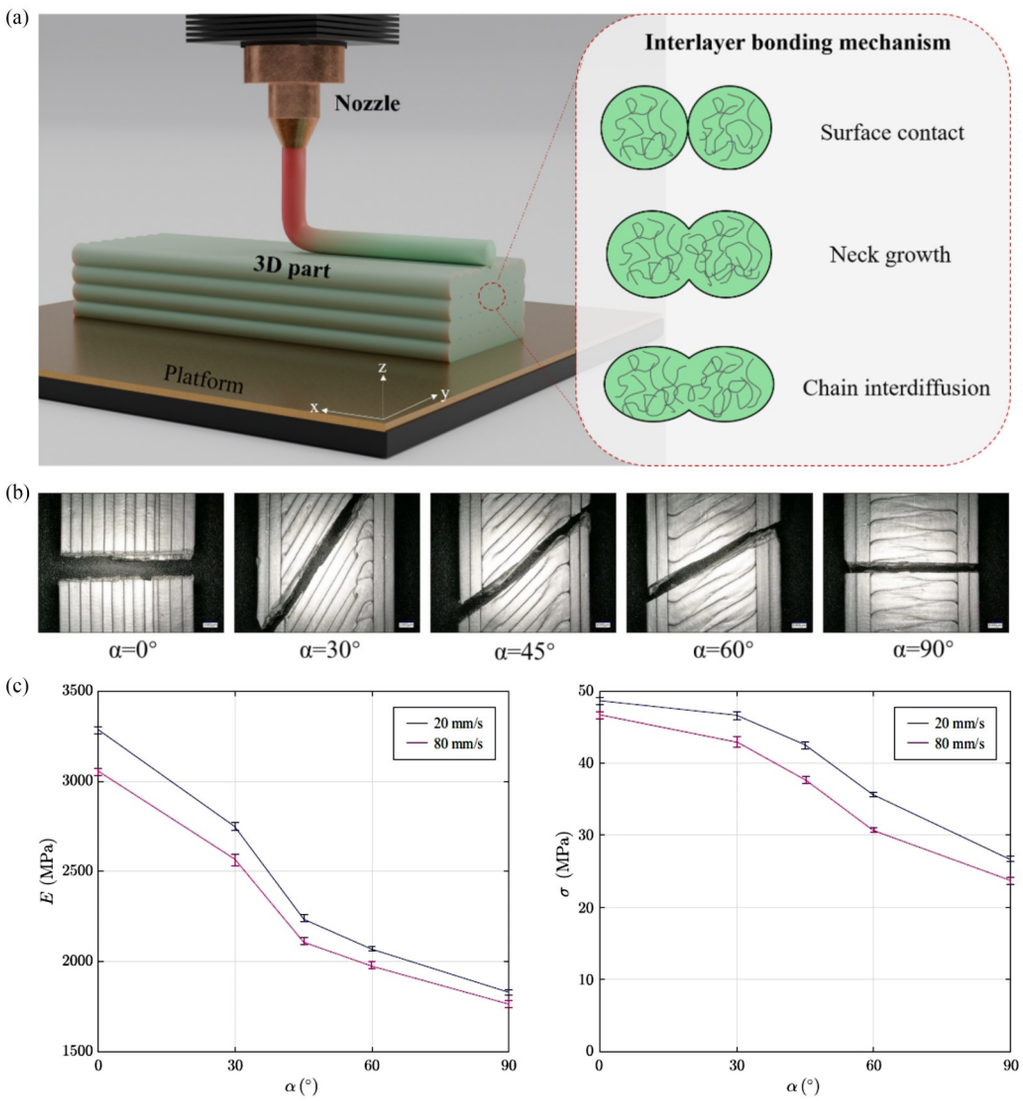


Fig. 3 Interlayer bonding ability of PLA material during FDM process: (a) schematic illustration of interlayer bonding mechanism during FFF process; (b) optical images of PLA specimens with different raster angles after failure; (c) dependence of Young's modulus (E) and tensile strength (σ) on the raster angles for FDM-printed PLA specimens (Reproduced from Ref. [65]; Copyright (2022) The Author(s), under the terms of the Creative Commons CC BY License).

度低于材料本体[64]. 这些薄弱结构作为应力集中点，诱使PLA打印件在较低应力下失效，并呈现显著的力学各向异性[65~68]. 由于层间界面薄弱，打印方向、填充角度等决定薄层与载荷相对方向的参数，直接影响PLA打印件的力学性能[69~71]. 例如，填充角度为0°的3D打印件因丝材本身平行于载荷方向而发生层内断裂(图3b)，其拉伸强度可达50 MPa，模量约为3.3 GPa[65]. 随着填充角度从0°变为45°，3D打印件的强度和弹性模量逐渐下降(图3c). 当打印方向为90°时，3D打印件在层间结合界面处断裂(图3b)，其拉伸强度仅为6~30 MPa[65,67]. 换言之，填充角度为90°的PLA打印件，其拉伸强度仅为0°样品的15%~60%[71]. 因此，增强层间界面结合是聚乳酸3D打印件强韧化的关键，也是当前的高性能聚乳酸3D打印材料的重要发展方向.

2 聚乳酸3D打印件的层间界面增强

本节将从材料、工艺及后处理等方面系统总结近年来围绕聚乳酸3D打印件的层间界面调控展开的一系列研究工作，并深入剖析其增强机理. 其中，材料改性是改善聚乳酸3D打印件层间界面性能最重要的手段之一[72,73]. 依据对层间界面作用机制的不同，材料改性策略可进一步分为物理改性与化学改性2类. 前者主要通过物理共混或复合调控PLA分子链运动能力或结晶行为，促进层间界面的黏性烧结与分子链互扩散，从而增强界面结合；后者则通过在PLA基体中引入活性官能团，使材料在特定条件下发生化学反应，在结合界面形成化学键

交联，从而有效增强其力学性能. 下面详细介绍不同策略在调控聚乳酸3D打印件层间界面结构、改善其力学性能方面的研究进展.

2.1 材料物理改性

当前，增强层间界面的策略之一是利用低分子量聚合物如聚乙二醇(PEG)、低分子量PLA及聚羟基脂肪酸酯等增塑PLA基体，增强PLA分子链运动能力，降低熔体黏度，促进薄层间的黏性烧结与分子链互扩散，进而提高3D打印件的力学性能[74,75]. 本课题组[76]研究了PEG对聚乳酸3D打印件的层间界面性能影响，发现分子量为8000 g/mol的PEG可以将层间结合强度提高至44 MPa，获得各向异性程度仅为16%的3D打印件. 上海交通大学Tong团队[77]在PLA基体中加入0.1 wt%超支化聚酯酰亚胺(HBPEIs)，以促进相邻薄层融合与界面分子链互扩散，再通过冷结晶进一步加强界面物理交联，将3D打印件的层间结合强度从23.1 MPa提升至46.6 MPa，力学各向异性程度降低至4.1%. 值得注意是，增塑剂对层间界面的增强效果依赖于其增塑效应与界面缠结效应之间的平衡，必须严格设计添加剂的分子量、支化度和添加量，才能在促进界面分子链快速扩散的同时，确保其链段长度足以与界面处PLA分子链发生缠结[74,75]. 否则，过量增塑剂或过低分子量增塑剂的加入将导致3D打印件相分离、表面迁移及本征力学性能急剧下降等问题.

向PLA基体中引入纳米粒子或增强纤维是构筑高性能复合材料的有效手段，但其对3D打印件层间界面性能的增强效果较差. 大多情况，增强填料加剧PLA打印件的孔隙率，降低层间结合强度[72,78~80]. 这是因为纤维或纳米粒子的加入会显著增加PLA黏度，不利于相邻薄层间的黏性烧结与分子链互扩散. 因此，由复合材料制成的3D打印件既有因层间结合不充分带来的介观孔隙，还存在填料/基体间的微纳米孔隙，它们在外载荷作用下作为应力集中点，诱导3D打印件在较低应力下失效[81]. 近期研究表明，调控纤维在3D打印件中的取向度，可在一定程度上增强层间界面. 当纤维素纳米纤维(CNFs)沿着层内单一取向时，聚乳酸3D打印件的层内模量和强度分别提高69.9%和68.2%，但其层间结合界面的强度和模量下降，导致力学各向差异高达64.7%~69.9%. 相比之下，任意三维取向的CNFs可将3D打印件的力学各向差异控制在8.2%~24.6%，使其在复杂载荷条件下表现出更好的力学稳定性[82].

值得注意的是，物理改性所引起的PLA结晶行为变化对其3D打印件层间结合强度起着不可忽视的影响. 如图4(a)所示，在喷嘴温度为210 ℃和底板温度为60 ℃的条件下打印纳米二氧化硅(SiO_2)/PLA复合材料时，纳米SiO_2加速PLA结晶，抑制层间界面分子链互扩散，导致3D打印件的层间界面强度降低；而当底板温度升高至80 ℃，复合材料的结晶速率变慢，分子链得以在层间界面处充分互扩散后再结晶，使界面模量和强度提高16.5%和23.0% (图4b)[78]. 本课题[55,83]研究发现，通过底板温度、退火温度的调控可控制PLA的结晶速率，进而影响3D打印件的层间结合强度. 如图4(c)所示，当底板温度或者退火温度高于90 ℃，PLA材料的半结晶时间小于其链段松弛时间，结晶显著地抑制了层间界面的分子链扩散，所得3D打印件中的层间结合强度低于15 MPa. 当底板温度低于70 ℃时，PLA的半结晶时间远超90 min，此时结晶对层间界面的分子链扩散影响较小，所得3D打印件的结晶度小于10%、且层间结合强度高达24.7 MPa[83].

可见，通过材料改性调控聚乳酸3D打印件的层间界面性能，需要综合考虑改性材料和打印工艺协同作用下的PLA结晶对界面处分子链互扩散的影响[62,84]. 也正因如此，调控结晶行为已成为增强聚乳酸3D打印件层间界面的新方法. Srinivas等[63]采用双喷头交替沉积PLLA和PDLA，在相邻丝材界面诱导立构复合结晶. 研究表明，较低分子量和较慢打印速度有利于链段跨界面扩散，提高立构复合晶体含量；形成的晶体网络可强化层间焊接区，并诱导本体进一步结晶. 与单一PLA打印件相比，交替打印PLA样品的储能模量提高约40%，同时有助于改善打印件的热力学稳定性和尺寸稳定性.

2.2 材料化学改性

与物理改性不同，材料化学改性法则是通过在PLA分子链上引入反应性基团，或在PLA基体中加入活性组分[85,86]，在一定打印条件下引发化学反应，有效改善PLA打印件的力学各向异性，并赋予其可逆修复性或智能响应性. Jubinville等[87]在PLA中加入一定量光引发剂和交联剂，制备成光活性打印材料，将其3D打印后进行紫外光辐照处理. 在紫外光照下，光引发剂促使PLA分子产生烷基自由基，引发交联剂的环氧基团开环，在层间界面形成化学交联网络，将层间结合强度提高64%. 浙江理工大学Zhang教授与浙江大学Fang教授团队[88]合成了2种巯基封端的硼酸酯：苯基硼酸酯(PB)和硼酸

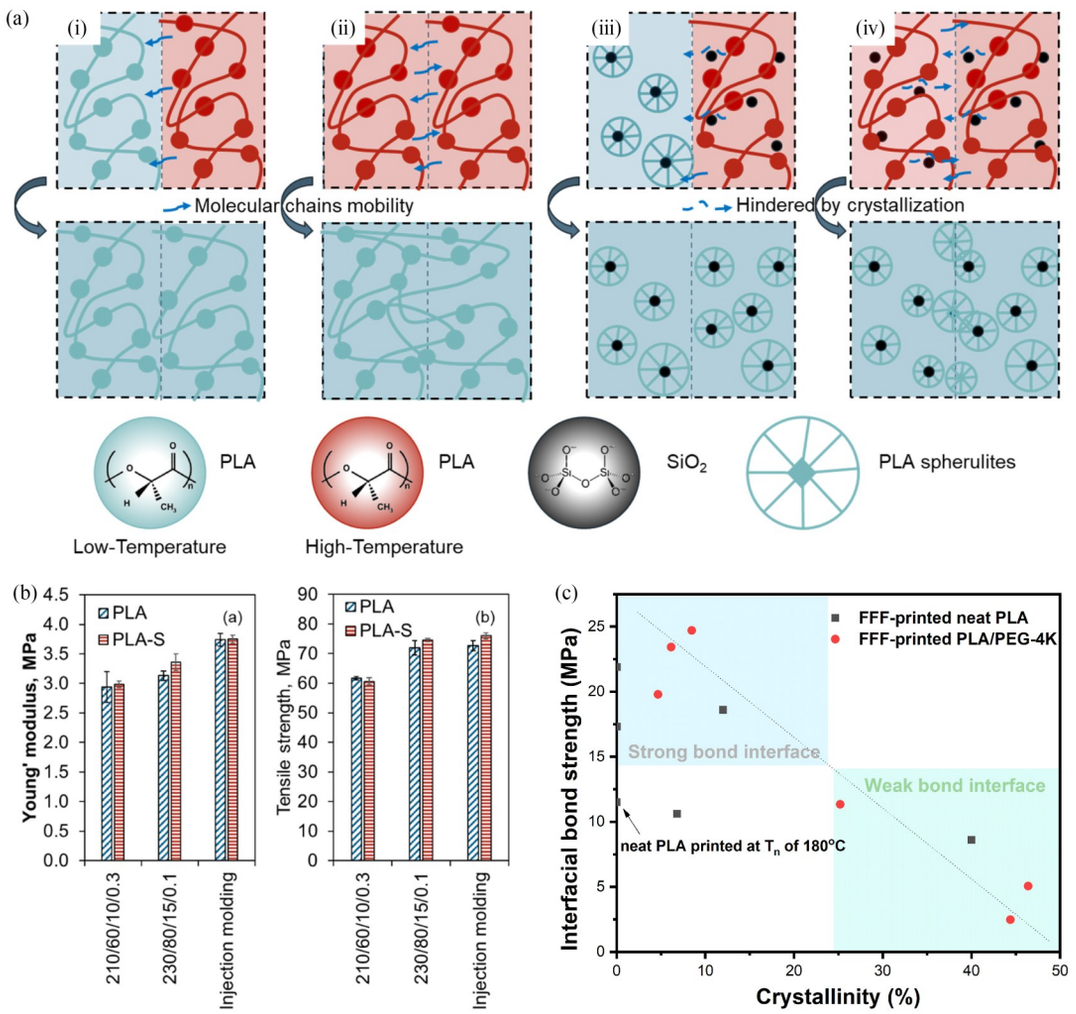


Fig. 4 Effect of crystallization on the interlayer bonding of FDM-printed PLA parts: (a) schematic illustration of the diffusion mechanisms in PLA (i, ii) and PLA-S (silica) (iii, iv) under different printing conditions; (b) Young's modulus and tensile strength of 3D printed- and injection-molded PLA and PLA-S under different printing conditions (Reproduced from Ref. [78]; Copyright (2025) The Author(s), under the terms of the Creative Commons CC BY License); (c) Interfacial bond strength as a function of crystallinity (Reprinted with permission from Ref. [83]; Copyright (2026) American Chemical Society).

阴离子(BA) (图5a)，将其与多烯烃在紫外光下通过硫醇–烯点击制成动态聚合物(图5b)，以改性PLA基体. 利用高温下这一动态聚合物的硼酸酯键的可逆交换特性，实现了PLA打印件的层间化学交联与分子链扩散的协同调控(图5c). 硼酸酯动态键的可逆性还赋予改性PLA模块化打印能力，可将复杂模型先分解为无支撑打印的子模块，分块打印后，在加热条件下通过界面化学愈合制备成复杂的蘑菇、高脚杯(图5d). 结合PLA基体的形状记忆效应，复杂模型可在弯曲后经加热恢复原状，实现了模块化4D打印. 硼酸酯交联剂对层间界面的增强效果受到硼酸酯种类与含量的影响(图5e). 含20% PB交联剂的PLA打印件在Z向的拉伸强度高达33.79 MPa，较纯PLA提升150%，同时其在X向的强度保持基本不变(图5f).

2.3 打印工艺优化

在FDM成型中，喷嘴温度、底板温度、打印速度及填充角度等工艺参数，直接决定了材料所经历的热历史与外场力，进而影响相邻薄层间的黏性烧结、分子链互扩散以及结晶等行为. 因此，优化工艺参数也是提升PLA打印件层间结合性能最常用的途径之一[89].

喷嘴温度是影响PLA打印件层间结合强度的关键工艺参数之一. 研究表明，当喷嘴温度从155 ℃升高至190 ℃时，层间结合强度可由6.8 MPa提高至28.2 MPa[90]. 这是因为，提高喷嘴温度能够有效降低PLA熔体黏度，加快熔体形成较大烧结颈，促进界面分子链扩散和缠结. 然而，过高的喷嘴温度可引发材料热降解，使熔体黏度急剧降低，导致3D打印件表面精度下降及力学性能劣化[91,92].

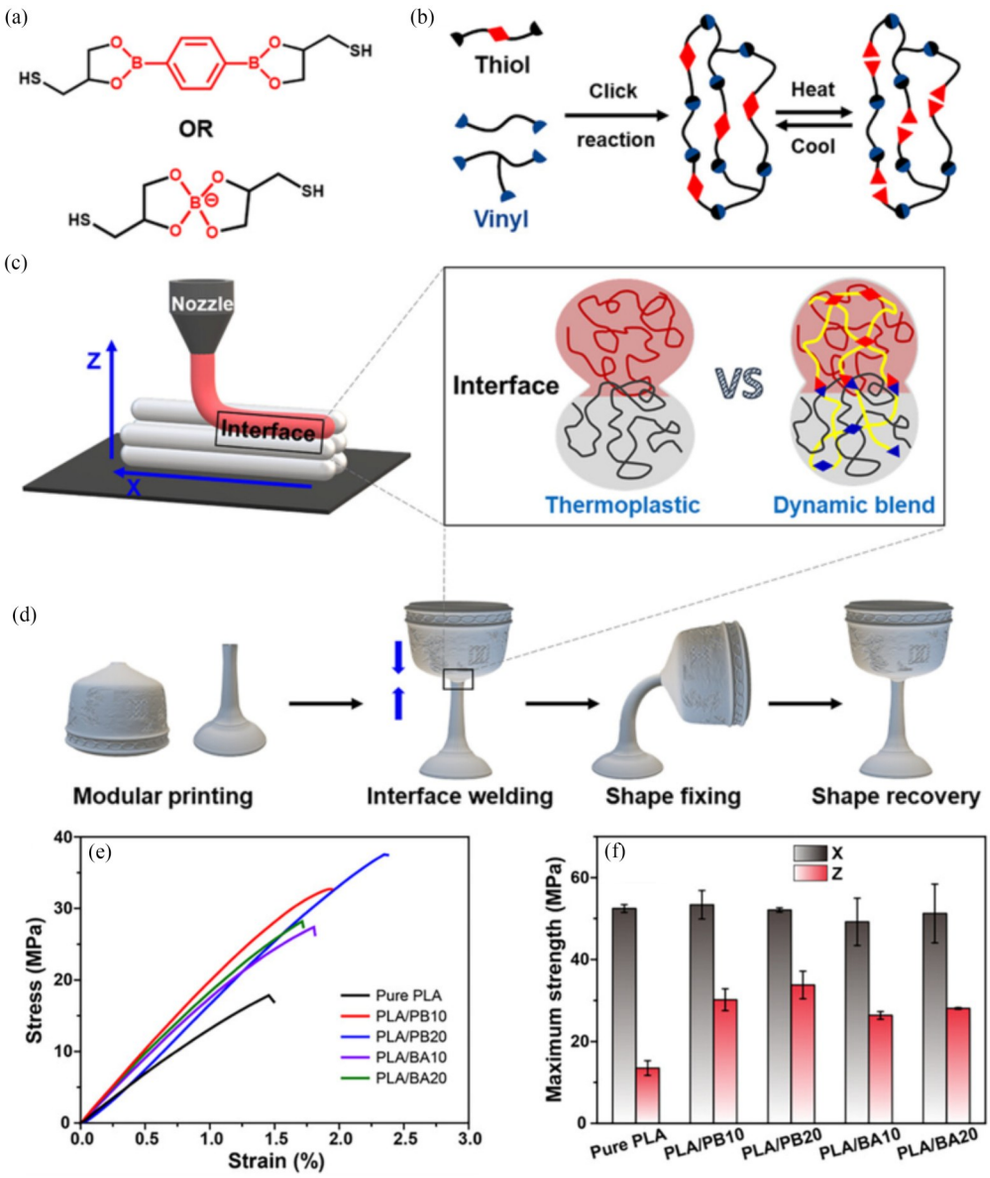


Fig. 5 Enhancement of interfacial bonding by dynamic chemistry network. (a) Molecular structures of dynamic PB and SA crosslinkers; (b) Dynamic network formed *via* click-reaction of PB and SA with vinyl; (c) Interfacial interactions for FFF-printed PLA parts containing PB or SA; (d) Modular 4D printing; (e) Stress-strain curves of printed PLA along the *Z*-axis direction and (f) mechanical strengths along the *X*- and *Z*-axis directions (Reprinted with permission from Ref. [88]; Copyright (2025) Wiley-VCH GmbH).

因此，喷嘴温度的选择，需在提升链段运动能力与保障材料热稳定性之间取得平衡.

此外，底板温度与成型腔体温度也会影响PLA熔体的冷却速率，决定其结晶动力学，进而影响3D打印件的层间结合强度及力学各向异性.将底板温度设定在略高于PLA玻璃化转变温度(T_g，约55~65 ℃)时，可减缓打印件底部的冷却速率，有效增强打印件底部区域的层间结合质量[93]. 但由于聚合物本身较低热传导能力，底板温度对远离底板的层间界面影响有限.相比之下，提高成型腔温度能均匀地调控各薄层温度，既延长熔体处于T_g以上的时间，为所有薄层结合界面处的分子链充分扩散、穿透与深度缠结提供热力学条件[94]，又通过恒温环境减小层间温度梯度、释放残余热应力，并适度调控结晶，大幅提升3D打印件的层间结合强度，降低力学各向异性[95].

其他参数，如层厚和打印速率也会影响3D打印件的层间结合性能.比如，较薄的层厚(0.1~0.2 mm)能够改善表面质量，减少层间空隙，提高层间结合强度，有效抑制裂纹的萌生和扩展.相反，较高的层厚会减少相邻薄层接触面积，引入孔隙、残余内应力等缺陷，降低层间结合质量，影响

3D打印件的整体力学性能[96,97]. 在较低打印速率下制备的PLA打印件的拉伸强度会有所提升，这得益于高温喷嘴在沉积薄层上停留的时间较长，能提高薄层温度，延长分子链扩散时间，减少孔隙率[90,91].

事实上，多种打印参数之间往往协同作用，共同影响着3D打印件的力学性能. Kumar等[98]结合Taguchi法建模、CRITIC嵌入的WASPAS多准则决策方法以及实验验证等手段，研究了层厚、打印速度和温度等工艺参数对3D打印件力学性能的影响. 当层厚为0.1 mm、打印速度为60 mm/s和喷嘴温度为200 ℃时，所制备的3D打印件层间界面性能最优，其抗拉强度为45.52 MPa，冲击强度达6.21 kJ/m^2. 由此可知，聚乳酸3D打印件的力学性能提升不能通过优化单一参数来实现，且打印参数的优化与选择需综合权衡打印效率与打印质量之间的平衡关系.

2.4 原位外场辅助打印或后处理

为改善3D打印件的层间结合性能、降低力学各向异性，研究者还发展出了多种原位外场辅助打印及后处理策略. 此类方法在不改变材料组分的前提下，通过在打印过程或对已成型的制件施加热、机械或化学处理，调控沉积薄层的温度场，影响层间烧结行为、分子链扩散及界面局部重熔，修复层间界面缺陷，有效提升3D打印件的层间结合与整体力学性能，具有广泛的材料适配性.

针对聚乳酸3D打印发展的原位外场辅助打印策略，有机械辅助压实、热场辅助、超声振动和等离子体处理等. 机械压制法将滚轮与喷嘴集成，在打印过程中由滚轮对挤出沉积丝施加压力，促进材料铺展并提高层间接触紧密度，从而增强层间结合性能[99]. 此外，原位等离子体处理可通过在聚合物表面引入反应性官能团，提高表面极性与润湿性，进而改善层间结合. 例如，多材料PLA/TPU打印件经等离子处理后，其最大剪切载荷提高了63%，表明层间结合得到有效强化[100]. 热场辅助技术通过在喷嘴附近集成激光[101]、红外线[102]、热风[103]、电阻丝[104]及微波[79]等热源，对沉积材料进行局部或整体加热，既延长层间界面处的分子链扩散与缠结时间，又缓解了温度梯度和由此带来的翘曲和开裂，从而同步改善3D打印件的层间结合质量、表面精度及整体力学性能. 激光可实现对沉积薄层的定向局部加热，但常需复杂组件，能耗和成本较高[105]. 相比之下，红外辅助加热的成本较低、工艺灵活，能即时加热特定区域，诱导材料局部重熔并减小温度梯度[102]. 经红外辅助加热的PLA打印件，其层间结合强度由20.3 MPa提升至33.8 MPa，断裂伸长率从2.7%增至6.7%[102].

与上述直接热源不同，微波和超声处理属于间接辅助加热策略，需借助功能填料(如碳纳米管，CNT)将微波需转化为3D打印件的局部热源，促进层间界面处的熔融和链段扩散，从而增强层间结合强度[79,106]. 超声振动辅助策略也被用于PLA基复合材料，可促进沉积层间润湿与融合、减少内部孔隙、改善增强颗粒(如羟基磷灰石，HA)的分散性，降低应力集中，从而显著减小力学各向异性. 对于填充角度为90°的试样，10 wt% HA-PLA和20 wt% HA-PLA在超声辅助打印下的最高拉伸强度分别达到46.24和43.03 MPa，较未处理样品分别提高87.7%和112.7%[72].

除原位辅助打印外，后处理亦是改善其层间结合质量的有效途径之一. 在适宜温度下的退火热处理，不仅显著改善层间结合质量，降低3D打印件内残余应力和孔隙缺陷，还能有效提升PLA打印件的结晶度和晶体完善度，进而同步提升力学性能与热稳定性. 值得注意是的，退火条件的选择建立在对层间界面处的结晶与分子链扩散之间的竞争关系的认识之上，否则会影响所得增强效果. Windheim等[69]发现在冷结晶温度(T_{cc})以下退火处理PLA打印件，能将层间结合强度从退火前的27.3 MPa提升至37 MPa；而在T_{cc}以上退火，虽能提高3D打印件的结晶度，但对内部孔隙率和层间结合强度的影响甚微. 通常，PLA的最佳退火温度范围为70~120 ℃[83,107].

3 结论与展望

聚乳酸(PLA)是目前FDM技术应用最广泛的材料之一，兼具良好的挤出流动性、较高的尺寸稳定性和优异的生物相容性. 然而，受逐层堆积工艺的限制，PLA在成型过程中因温度急剧下降，熔体黏度升高、分子链运动能力受限，而表现出薄弱的层间结合质量，致使3D打印件的力学性能普遍低于传统加工件，并呈现明显的力学各向异性. 这一问题已成为制约PLA打印件从模型制造向承载结构及功能部件拓展应用的关键瓶颈.

聚乳酸3D打印件的力学各向异性本质上源于层间界面处黏性烧结及分子链互扩散/缠结的不充分，这一过程由界面处分子链运动能力与结晶速率的共同决定，而两者又随着材料所经历温度场和剪

切场而发生显著变化. 因此，当前改善PLA层间结合质量的策略，多通过材料物理改性、打印工艺优化、外场辅助打印及后处理等方式增强分子链运动能力. 不同策略均可在一定程度上改善PLA打印件的强度、刚度与韧性，并降低其力学各向异性. 但多数方法存在适用范围有限、打印成本增加等问题，为制备高强高韧、低各向异性聚乳酸3D打印件带来了诸多挑战.

未来将围绕以下几个方面展开系统深入研究：(1) 借助微聚焦表征(如X射线、红外等)手段，原位研究PLA在3D打印过程中的微观结构演变规律，揭示PLA结晶与层间结合等过程的耦合机制，剖析层间界面结构形成机理，建立层间界面微观结构与宏观力学之间的构效关系，为低各向异性PLA打印材料设计、工艺优化与后处理条件选择提供理论依据. (2) 基于PLA复合材料流变行为的系统研究与认识，构建兼具优异挤出流动性、较高尺寸精度与良好层间结合能力的功能性聚乳酸复合3D打印材料体系，摆脱传统依赖大量试错的配方开发模式，系统解决无机填料引入所导致的喷嘴堵塞与界面缺陷增加，以及大量增塑剂使用所带来的表面精度下降和本体性能劣化等关键问题. (3) 研究打印参数、外场辅助及后处理对层间结合和跨层结晶所起的作用，结合AI数据驱动、数值模拟与实验手段，建立面向不同PLA材料体系的工艺优化方法，实现多参数协同调控，制备综合性能优异的3D打印件. (4) 发挥PLA的形状记忆特性，结合3D打印技术在结构设计自由度高的优势，将材料改性与仿生结构设计相结合，通过多尺度协同设计，实现集轻量化、高性能与智能化于一身的聚乳酸3D打印.

总之，聚乳酸3D打印件的力学各向异性调控，正在由经验性参数优化逐步转向材料、工艺与结构的协同设计. 随着对层间结合机理认识的深化及多尺度结构调控方法的发展，构建兼具优异打印性、力学强韧性、智能响应性的PLA打印材料将成为未来的重要发展方向，也将为聚乳酸材料在高性能、绿色化和功能化增材制造领域的应用拓展提供有力支撑.

致谢

本研究由中国科学院中奥国际合作项目(项目号 027GJHZ2025060MI)和中央高校基本科研业务费专项资金(项目号 2682025CX126)资助.

REFERENCES

1 Heinze, D. A.; Das, A.; Williams, C. B.; McIlroy, C.; Peterson, A. M.; Bortner, M. J. Realizing semicrystalline polymer physics across disparate processing scales: from desktop extrusion to large-format additive manufacturing. *Prog. Polym. Sci.*, **2026**, 172, 102053.

2 Vidakis, N.; Petousis, M.; Spyridaki, M.; Mountakis, N.; Dimitriou, E.; Michailidis, N. Ultra- and high-performance polymers for material extrusion additive manufacturing: recent advancements, challenges, and optimization perspectives. *Mater. Sci. Eng. R Rep.*, **2026**, 167, 101086.

3 Wu, H.; Fahy, W. P.; Kim, S.; Kim, H.; Zhao, N.; Pilato, L.; Kafi, A.; Bateman, S.; Koo, J. H. Recent developments in polymers/polymer nanocomposites for additive manufacturing. *Prog. Mater. Sci.*, **2020**, 111, 100638.

4 Munshi, G. A.; Kulkarni, V. M. Polymer-based functionally graded multi-material additive manufacturing *via* material extrusion: interfacial mechanisms and gradient design strategies. *Next Mater.*, **2026**, 12, 102118.

5 Darnal, A.; Shahid, Z.; Deshpande, H.; Kim, J.; Muliana, A. Tuning mechanical properties of 3D printed composites with PLA: TPU programmable filaments. *Compos. Struct.*, **2023**, 318, 117075.

6 Goh, G. D.; Wong, K. K.; Jaw, W. Q.; Gobi, R.; Vellayappan, M. V.; Goh, Y. J. J.; Goh, G. L.; Seet, H. L.; Yeong, W. Y.; Nai, M. L. S. Exploring PLA/TPU blends in pellet-based printing for multifunctional applications: blending and interfacial properties. *Mater. Sci. Eng. R Rep.*, **2025**, 164, 100981.

7 Kumar, V.; Hassen, A. A.; Kunc, V.; Nuttall, D.; Kircaliali, A.; Talabi, S. I.; Reynolds, J.; Vaughan, J.; Mhatre, P.; Smith, T.; Šeta, B.; Spangenberg, J.; Blue, C. Genesis of a novel high-rate composite manufacturing process using large-scale additive manufacturing-compression molding (AM-CM) system: possibilities and limitations. *Compos. Part B Eng.*, **2026**, 309, 113101.

8 余生泉, 刘晨露, 徐翔民, 宗胡曾, 刘保英, 丁涛, 徐元清, 房晓敏, 鲁哲宏. 3D打印技术及其多领域应用研究进展. 高分子通报, **2026**, 39(7), 1091−1107.

9 Eryildiz, M.; Karakus, A.; Demirci, M.; Altintas Kadirhan, O.; Eksi Altan, M. Optimization of thermal, mechanical, biodegradation, and shape memory properties in 4D-printed PLA/PCL blends for spinal cages. *Polym. Adv. Technol.*, **2025**, 36(3), e70133.

10 Makki, T.; Vattathurvalappil, S. H.; Theravalappil, R.; Nazir, A.; Alhajeri, A.; Azeem, M. A.; Mahdi, E.; Ummer, A. C.; Ali, U. 3D and 4D printing: a review of virgin polymers used in fused deposition modeling. *Compos. Part C Open Access*, **2024**, 14, 100472.

11 赵丽萍, 段晓. 基于熔融沉积成型3D打印的聚乳酸/*β*-磷酸三钙复合医用多孔骨支架的制备与性能. 高分子通报, **2026**, 39(6), 967−975.

12 Huang, Y. J.; Mao, Y. F.; Li, H. F.; Wang, E. Y.; Mai, H. M.; Zhang, W. J.; Wen, J. M.; You, H.; Long, Y.; Guo, W.; Liu, B.; Wang, S. 3D-printed thermally activated shape memory PLA/TBC composite scaffold with body-compatible temperature for minimally invasive bone repair. *ACS Appl. Polym. Mater.*, **2025**, 7(7), 4572−4583.

13 de Albuquerque, T. L.; Marques, J. E. Jr, de Queiroz, L. P.; Ricardo, A. D. S.; Rocha, M. V. P. Polylactic acid production from biotechnological routes: a review. *Int. J. Biol. Macromol.*, **2021**, 186, 933−951.

14 Muthe, L. P.; Pickering, K.; Gauss, C. A review of 3D/4D printing of poly-lactic acid composites with bio-derived reinforcements. *Compos. Part C*, **2022**, 8, 100271.

15 Liu, Z. G.; Wang, Y. Q.; Wu, B. C.; Cui, C. Z.; Guo, Y.; Yan, C. A critical review of fused deposition modeling 3D printing technology in manufacturing polylactic acid parts. *Int. J. Adv. Manuf. Technol.*, **2019**, 102(9), 2877−2889.

16 Dubinenko, G.; Zinoviev, A.; Bolbasov, E.; Kozelskaya, A.; Shesterikov, E.; Novikov, V.; Tverdokhlebov, S. Highly filled poly(l-lactic acid)/hydroxyapatite composite for 3D printing of personalized bone tissue engineering scaffolds. *J. Appl. Polym. Sci.*, **2021**, 138(2), 49662.

17 Arif, Z. U.; Khalid, M. Y.; Noroozi, R.; Sadeghianmaryan, A.; Jalalvand, M.; Hossain, M. Recent advances in 3D-printed polylactide and polycaprolactone-based biomaterials for tissue engineering applications. *Int. J. Biol. Macromol.*, **2022**, 218, 930−968.

18 Duty, C.; Ajinjeru, C.; Kishore, V.; Compton, B.; Hmeidat, N.; Chen, X.; Liu, P.; Hassen, A. A.; Lindahl, J.; Kunc, V. What makes a material printable? A viscoelastic model for extrusion-based 3D printing of polymers. *J. Manuf. Process.*, **2018**, 35, 526−537.

19 Sola, A. Materials requirements in fused filament fabrication: a framework for the design of next-generation 3D printable thermoplastics and composites. *Macromol. Mater. Eng.*, **2022**, 307(10), 2200197.

20 Khouri, N. G.; Bahú, J. O.; Blanco-Llamero, C.; Severino, P.; Concha, V. O. C.; Souto, E. B. Polylactic acid (PLA): properties, synthesis, and biomedical applications-a review of the literature. *J. Mol. Struct.*, **2024**, 1309, 138243.

21 Vaes, D.; Van Puyvelde, P. Semi-crystalline feedstock for filament-based 3D printing of polymers. *Prog. Polym. Sci.*, **2021**, 118, 101411.

22 Castro-Aguirre, E.; Iñiguez-Franco, F.; Samsudin, H.; Fang, X.; Auras, R. Poly(lactic acid): mass production, processing, industrial applications, and end of life. *Adv. Drug Deliv. Rev.*, **2016**, 107, 333−366.

23 Phan, D. D.; Horner, J. S.; Swain, Z. R.; Beris, A. N.; MacKay, M. E. Computational fluid dynamics simulation of the melting process in the fused filament fabrication additive manufacturing technique. *Add. Manuf.*, **2020**, 33, 101161.

24 Das, A.; Gilmer, E. L.; Biria, S.; Bortner, M. J. Importance of polymer rheology on material extrusion additive manufacturing: correlating process physics to print properties. *ACS Appl. Polym. Mater.*, **2021**, 3(3), 1218−1249.

25 Rau, D. A.; Williams, C. B.; Bortner, M. J. Rheology and printability: a survey of critical relationships for direct ink write materials design. *Prog. Mater. Sci.*, **2023**, 140, 101188.

26 Torabi, H.; McGreal, H.; Zarrin, H.; Behzadfar, E. Effects of rheological properties on 3D printing of poly(lactic acid) (PLA) and poly(hydroxy alkenoate) (PHA) hybrid materials. *ACS Appl. Polym. Mater.*, **2023**, 5(6), 4034−4044.

27 Gao, X.; Zhang, D. J.; Qi, S. X.; Wen, X. N.; Su, Y. L. Mechanical properties of 3D parts fabricated by fused deposition modeling: effect of various fillers in polylactide. *J. Appl. Polym. Sci.*, **2019**, 136(31), 47824.

28 de Vries, S.; Schuller, T.; Galindo-Rosales, F. J.; Fanzio, P. Pressure drop non-linearities in material extrusion additive manufacturing: a novel approach for pressure monitoring and numerical modeling. *Addit. Manuf.*, **2024**, 80, 103966.

29 Arrigo, R.; Frache, A. FDM printability of PLA based-materials: the key role of the rheological behavior. *Polymers*, **2022**, 14(9), 1754.

30 Schuller, T.; Jalaal, M.; Fanzio, P.; Galindo-Rosales, F. J. Optimal shape design of printing nozzles for extrusion-based additive manufacturing. *Addit. Manuf.*, **2024**, 84, 104130.

31 Gilmer, E. L.; Miller, D.; Chatham, C. A.; Zawaski, C.; Fallon, J. J.; Pekkanen, A.; Long, T. E.; Williams, C. B.; Bortner, M. J. Model analysis of feedstock behavior in fused filament fabrication: enabling rapid materials screening. *Polymer*, **2018**, 152, 51−61.

32 Wu, J. T.; Chen, N.; Wang, Q. Preparation of novel thermoplastic poly(vinyl alcohol) with improved processability for fused deposition modeling. *Polym. Adv. Technolog.*, **2018**, 29(5), 1447−1455.

33 Farah, S.; Anderson, D. G.; Langer, R. Physical and mechanical properties of PLA, and their functions in widespread applications: a comprehensive review. *Adv. Drug Deliv. Rev.*, **2016**, 107, 367−392.

34 Colon, A. R.; Kazmer, D. O.; Peterson, A. M.; Seppala, J. E. Characterization of die-swell in thermoplastic material extrusion. *Addit. Manuf.*, **2023**, 73, 103700.

35 Mbow, M. M.; Marin, P. R.; Pourroy, F. Extruded diameter dependence on temperature and velocity in the fused deposition modeling process. *Prog. Addit. Manuf.*, **2020**, 5(2), 139−152.

36 Pibulchinda, P.; Barocio, E.; Favaloro, A. J.; Pipes, R. B. Influence of printing conditions on the extrudate shape and fiber orientation in extrusion deposition additive manufacturing. *Compos. Part B Eng.*, **2023**, 261, 110793.

37 Tang, T. O.; Holmes, S.; Dean, K.; Simon, G. P. Design and fabrication of transdermal drug delivery patch with milliprojections using material extrusion 3D printing. *J. Appl. Polym. Sci.*, **2020**, 137(23), 48777.

38 Sirisinha, C. A review of extrudate swell in polymers. *ScienceAsia*, **1997**, 23(4), 259−280.

39 Bian, Y. H.; Yu, G.; Zhao, X.; Li, S. X.; He, X. L.; Tian, C. X.; Li, Z. Y. Exit morphology and mechanical property of FDM printed PLA: influence of hot melt extrusion process. *Adv. Manuf.*, **2023**, 11(1), 56−74.

40 Bakrani Balani, S.; Chabert, F.; Nassiet, V.; Cantarel, A. Influence of printing parameters on the stability of deposited beads in fused filament fabrication of poly(lactic) acid. *Addit. Manuf.*, **2019**, 25, 112−121.

41 Patti, A.; Acierno, S.; Cicala, G.; Acierno, D. Predicting the printability of poly(lactide) acid filaments in fused deposition modeling (FDM) technology: rheological measurements and experimental evidence. *ChemEngineering*, **2023**, 7(1), 1.

42 Calafel, M. I.; Pérez-Camargo, R.; Aguirresarobe, R.; Candal, M. V.; Müller, A. J. Additive manufacturing of semicrystalline polymers: understanding structural integrity and dimensional accuracy. in *Additive Manufacturing of Functional Polymers and Nanocomposites*. Amsterdam: Elsevier, **2025**, p.3−51.

43 Spoerk, M.; Holzer, C.; Gonzalez-Gutierrez, J. Material extrusion-based additive manufacturing of polypropylene: a review on how to improve dimensional inaccuracy and warpage. *J. Appl. Polym. Sci.*, **2020**, 137(12), 48545.

44 Algarni, M.; Ghazali, S. Comparative study of the sensitivity of PLA, ABS, PEEK, and PETG's mechanical properties to FDM printing process parameters. *Crystals*, **2021**, 11(8), 995.

45 Martins, R. F.; Branco, R.; Martins, M.; Macek, W.; Marciniak, Z.; Silva, R.; Trindade, D.; Moura, C.; Franco, M.; Malça, C. Mechanical properties of additively manufactured polymeric materials: PLA and PETG: for biomechanical applications. *Polymers*, **2024**, 16(13), 1868.

46 Torrado, A. R.; Shemelya, C. M.; English, J. D.; Lin, Y. R.; Wicker, R. B.; Roberson, D. A. Characterizing the effect of additives to ABS on the mechanical property anisotropy of specimens fabricated by material extrusion 3D printing. *Addit. Manuf.*, **2015**, 6, 16−29.

47 Xin, K.; Wei, Y.; Xiong, J. X.; Ni, Y. P.; Wang, X. F.; Xu, Y. J. Simultaneous strengthening and toughening of PLA with full recyclability enabled by resin-microsphere-modified L-lactide oligomers. *Chem. Eng. J.*, **2024**, 500, 156743.

48 Ullah, I.; Wasif, M.; Tufail, M. Analysis of shrinkage and dimensional accuracy of additively manufactured tooling for the composite manufacturing. *Int. J. Interact. Des. Manuf. Ijidem*, **2024**, 18(2), 673−684.

49 Buj-Corral, I.; Zayas-Figueras, E. E. Comparative study about dimensional accuracy and form errors of FFF printed spur gears using PLA and nylon. *Polym. Test.*, **2023**, 117, 107862.

50 Harris, A. M.; Lee, E. C. Improving mechanical performance of injection molded PLA by controlling crystallinity. *J. Appl. Polym. Sci.*, **2008**, 107(4), 2246−2255.

51 Sattler, R.; Zhang, R.; Gupta, G.; Du, M. X.; Runge, P. M.; Altenbach, H.; Androsch, R.; Beiner, M. Influence of crystallization kinetics and flow behavior on structural inhomogeneities in 3D-printed parts made from semi-crystalline polymers. *Macromolecules*, **2024**, 57(7), 3066−3080.

52 Salmerón Sánchez, M.; Mathot, V. B. F.; Vanden Poel, G.; Gómez Ribelles, J. L. Effect of the cooling rate on the nucleation kinetics of poly(l-lactic acid) and its influence on morphology. *Macromolecules*, **2007**, 40(22), 7989−7997.

53 Kothavade, P.; Yadav, P.; Gopal, A.; Pol, H.; Kafi, A.; Bateman, S.; Shanmuganathan, K. Enhancing the crystallization kinetics and mechanical properties of poly(lactic acid) blends for 3D printing application. *ACS Appl. Polym. Mater.*, **2024**, 6(10), 5754−5762.

54 Seppala, J. E.; Migler, K. D. Infrared thermography of welding zones produced by polymer extrusion additive manufacturing. *Addit. Manuf.*, **2016**, 12, 71−76.

55 Gao, X.; Qi, S. X.; Yang, B.; Su, Y. L.; Li, J.; Wang, D. J. Synergistic effect of plasticizer and nucleating agent on crystallization behavior of polylactide during fused filament fabrication. *Polymer*, **2021**, 215, 123426.

56 Abeykoon, C.; Sri-Amphorn, P.; Fernando, A. Optimization of fused deposition modeling parameters for improved PLA and ABS 3D printed structures. *Int. J. Light. Mater. Manuf.*, **2020**, 3(3), 284−297.

57 Hanon, M. M.; Zsidai, L.; Ma, Q. J. Accuracy investigation of 3D printed PLA with various process parameters and different colors. *Mater. Today Proc.*, **2021**, 42, 3089−3096.

58 Gendviliene, I.; Simoliunas, E.; Rekstyte, S.; Malinauskas, M.; Zaleckas, L.; Jegelevicius, D.; Bukelskiene, V.; Rutkunas, V. Assessment of the morphology and dimensional accuracy of 3D printed PLA and PLA/HAp scaffolds. *J. Mech. Behav. Biomed. Mater.*, **2020**, 104, 103616.

59 Pang, R.; Lai, M. K.; Ismail, K. I.; Yap, T. C. Characterization of the dimensional precision, physical bonding, and tensile performance of 3D-printed PLA parts with different printing temperature. *J. Manuf. Mater. Process.*, **2024**, 8(2), 56.

60 Ergene, B.; İnci, Y. E.; Çetintaş, B.; Daysal, B. An experimental study on the wear performance of 3D printed polylactic acid and carbon fiber reinforced polylactic acid parts: effect of infill rate and water absorption time. *Polym. Compos.*, **2025**, 46(1), 372−386.

61 Gao, X.; Qi, S. X.; Kuang, X.; Su, Y. L.; Li, J.; Wang, D. J. Fused filament fabrication of polymer materials: a review of interlayer bond. *Addit. Manuf.*, **2021**, 37, 101658.

62 Srinivas, V.; van Hooy-Corstjens, C. S. J.; Rastogi, S.; Harings, J. A. W. Promotion of molecular diffusion and/or crystallization in fused deposition modeled poly(lactide) welds. *Polymer*, **2020**, 202, 122637.

63 Srinivas, V.; van Hooy-Corstjens, C. S. J.; Vaughan, G. B. M.; van Leeuwen, B.; Rastogi, S.; Harings, J. A. W. Interfacial stereo complexation to strengthen fused deposition modeled poly(lactide) welds. *ACS Appl. Polym. Mater.*, **2019**, 1(8), 2131−2139.

64 Shmueli, Y.; Jiang, J. L.; Zhou, Y. C.; Xue, Y.; Chang, C. C.; Yuan, G. C.; Satija, S. K.; Lee, S.; Nam, C. Y.; Kim, T.; Marom, G.; Gersappe, D.; Rafailovich, M. H. Simultaneous *in situ* X-ray scattering and infrared imaging of polymer extrusion in additive manufacturing. *ACS Appl. Polym. Mater.*, **2019**, 1(6), 1559−1567.

65 Khosravani, M. R.; Berto, F.; Ayatollahi, M. R.; Reinicke, T. Characterization of 3D-printed PLA parts with different raster orientations and printing speeds. *Sci. Rep.*, **2022**, 12, 1016.

66 Wang, S. H.; Ma, Y. B.; Deng, Z. C.; Zhang, S.; Cai, J. X. Effects of fused deposition modeling process parameters on tensile, dynamic mechanical properties of 3D printed polylactic acid materials. *Polym. Test.*, **2020**, 86, 106483.

67 Karimi, H. R.; Khedri, E.; Nazemzadeh, N.; Mohamadi, R. Effect of layer angle and ambient temperature on the mechanical and fracture characteristics of unidirectional 3D printed PLA material. *Mater. Today Commun.*, **2023**, 35, 106174.

68 Murali, A.; Vakkattil, M. A.; Parameswaran, R. Investigating the effect of processing parameters on mechanical behavior of 3D fused deposition modeling printed polylactic acid. *J. Mater. Eng. Perform.*, **2023**, 32(3), 1089−1102.

69 von Windheim, N.; Collinson, D. W.; Lau, T.; Brinson, L. C.; Gall, K. The influence of porosity, crystallinity and interlayer adhesion on the tensile strength of 3D printed polylactic acid (PLA). *Rapid Prototyp. J.*, **2021**, 27(7), 1327−1336.

70 Kiendl, J.; Gao, C. Controlling toughness and strength of FDM 3D-printed PLA components through the raster layup. *Compos. Part B Eng.*, **2020**, 180, 107562.

71 Doshi, M.; Mahale, A.; Kumar Singh, S.; Deshmukh, S. Printing parameters and materials affecting mechanical properties of FDM-3D printed parts: perspective and prospects. *Mater. Today Proc.*, **2022**, 50, 2269−2275.

72 Aihemaiti, P.; Jiang, H. F.; Aiyiti, W.; Wang, J.; Dong, L. L.; Shuai, C. J. Mechanical properties enhancement of 3D-printed HA-PLA composites using ultrasonic vibration assistance. *Virtual Phys. Prototyp.*, **2024**, 19(1), e2346271.

73 Jiang, Z.; Diggle, B.; Tan, M. L.; Viktorova, J.; Bennett, C. W.; Connal, L. A. Extrusion 3D printing of polymeric materials with advanced properties. *Adv. Sci.*, **2020**, 7(17), 2001379.

74 Levenhagen, N. P.; Dadmun, M. D. Interlayer diffusion of surface segregating additives to improve the isotropy of fused deposition modeling products. *Polymer*, **2018**, 152, 35−41.

75 Levenhagen, N. P.; Dadmun, M. D. Bimodal molecular weight samples improve the isotropy of 3D printed polymeric samples. *Polymer*, **2017**, 122, 232−241.

76 Gao, X.; Qi, S. X.; Zhang, D. J.; Su, Y. L.; Wang, D. J. The role of poly(ethylene glycol) on crystallization, interlayer bond and mechanical performance of polylactide parts fabricated by fused filament fabrication. *Addit. Manuf.*, **2020**, 35, 101414.

77 Yang, X. Y.; Liu, Z. D.; Jing, H. T.; Zhang, C. Y.; He, Z. D.; Tong, G. S.; Zhu, X. Y. Enhanced interlayer adhesion of 3D printed poly(lactide acid) with ultralow hyperbranched poly(ester imide)s. *Compos. Commun.*, **2024**, 48, 101927.

78 Xu, Y.; Lin, L. Y.; Schlarb, A. K. Simulation-supported optimization of interlayer diffusion and crystallization in nanosilica-reinforced polylactic acid (PLA) manufactured by material extrusion. *Polymer*, **2025**, 337, 129009.

79 Li, H. F.; Mu, Y. X.; Wang, Q.; Cai, D. D.; Zhang, Y.; Luo, Y.; Liu, J.; Liu, J. T.; Niu, K. M.; Wu, Y.; Li, Y. Z.; Jiang, N. S. Interlayer enhancement of 3D printed CF/PLA composites *via* localized microwave welding and annealing-induced crystallization. *Compos. Part B Eng.*, **2024**, 284, 111737.

80 Jiang, D. L.; Smith, D. E. Anisotropic mechanical properties of oriented carbon fiber filled polymer composites produced with fused filament fabrication. *Addit. Manuf.*, **2017**, 18, 84−94.

81 Mohan, N.; Senthil, P.; Vinodh, S.; Jayanth, N. A review on composite materials and process parameters optimisation for the fused deposition modelling process. *Virtual Phys. Prototyp.*, **2017**, 12(1), 47−59.

82 Luo, C.; Kogakura, T.; Lee, C. E.; Huang, Y. H.; Uetsuji, Y. Multiscale study on mechanical anisotropy and interfacial behavior of 3D printed biodegradable polymer composites. *Compos. Struct.*, **2026**, 379, 119948.

83 Huang, C. X.; Zhang, H.; Yao, Y.; Chen, Y.; Huang, Y. Y.; Sun, D. X.; Chen, K. J.; Gao, X.; Su, Y. L. Regulating crystallization to enhance interfacial bonding in material-extrusion 3D printed polylactic acid parts. *Macromolecules*, **2026**, 59(17), 9308−9320.

84 Srinivas, V.; van Hooy-Corstjens, C. S. J.; Harings, J. A. W. Correlating molecular and crystallization dynamics to macroscopic fusion and thermodynamic stability in fused deposition modeling; a model study on polylactides. *Polymer*, **2018**, 142, 348−355.

85 Sharma, A.; Chand, A.; Singh, I.; Gaur, B. Vitrimers for 3D printing technology: current status and future perspectives. *Ind. Eng. Chem. Res.*, **2025**, 64(5), 2491−2515.

86 Yang, K. J.; Grant, J. C.; Lamey, P.; Joshi-Imre, A.; Lund, B. R.; Smaldone, R. A.; Voit, W. Diels-Alder reversible thermoset 3D printing: isotropic thermoset polymers *via* fused filament fabrication. *Adv. Funct. Mater.*, **2017**, 27(24), 1700318.

87 Jubinville, D.; Mekonnen, T. H. Enhanced performance 3D printed PLA parts through a photo-initiator mediated UV-curing. *Adv. Mater. Technolog.*, **2025**, 10(14), 2500124.

88 Peng, W. J.; Xia, H. X.; Wu, J. J.; Fang, Z. Z.; Zhang, X. M. Dynamic boronate ester chemistry facilitating 3D printing interlayer adhesion and modular 4D printing of polylactic acid. *Adv. Funct. Mater.*, **2025**, 35(25), 2503682.

89 Ali Ali, M. Y.; Rao, G. K. M.; Prasad, B. A. Multi-criteria optimization of 3D printing parameters for polylactic acid (PLA). *Prog. Addit. Manuf.*, **2025**, 10(12), 10855−10869.

90 Carlier, E.; Marquette, S.; Peerboom, C.; Denis, L.; Benali, S.; Raquez, J. M.; Amighi, K.; Goole, J. Investigation of the parameters used in fused deposition modeling of poly(lactic acid) to optimize 3D printing sessions. *Int. J. Pharm.*, **2019**, 565, 367−377.

91 Chen, K.; Yu, L. G.; Cui, Y. H.; Jia, M. Y.; Pan, K. Optimization of printing parameters of 3D-printed continuous glass fiber reinforced polylactic acid composites. *Thin Walled Struct.*, **2021**, 164, 107717.

92 Gajjar, T.; Yang, R.; Ye, L.; Zhang, Y. X. Effects of key process parameters on tensile properties and interlayer bonding behavior of 3D printed PLA using fused filament fabrication. *Prog. Addit. Manuf.*, **2025**, 10(2), 1261−1280.

93 Costa, S. F.; Duarte, F. M.; Covas, J. A. Thermal conditions affecting heat transfer in FDM/FFE: a contribution towards the numerical modelling of the process: this paper investigates convection, conduction and radiation phenomena in the filament deposition process. *Virtual Phys. Prototyp.*, **2015**, 10(1), 35−46.

94 McIlroy, C.; Olmsted, P. D. Disentanglement effects on welding behaviour of polymer melts during the fused-filament-fabrication method for additive manufacturing. *Polymer*, **2017**, 123, 376−391.

95 Thumsorn, S.; Prasong, W.; Ishigami, A.; Kurose, T.; Kobayashi, Y.; Ito, H. Influence of ambient temperature and crystalline structure on fracture toughness and production of thermoplastic by enclosure FDM 3D printer. *J. Manuf. Mater. Process.*, **2023**, 7(1), 44.

96 Ghaffar, A.; Riaz, M. T.; Rehman, A.; Sayed Al Mahmud, M. M. An optimized 3D printer by enhancing material properties and surface finish of PLA through modifications. *J. Eng.*, **2024**, 2024(1), 9198329.

97 Morvayová, A.; Contuzzi, N.; Casalino, G. Defects and residual stresses finite element prediction of FDM 3D printed wood/PLA biocomposite. *Int. J. Adv. Manuf. Technol.*, **2023**, 129(5), 2281−2293.

98 Kumar, M. S.; Farooq, M. U.; Ross, N. S.; Yang, C. H.; Kavimani, V.; Adediran, A. A. Achieving effective interlayer bonding of PLA parts during the material extrusion process with enhanced mechanical properties. *Sci. Rep.*, **2023**, 13(1), 6800.

99 Ravoori, D.; Salvi, S.; Prajapati, H.; Qasaimeh, M.; Adnan, A.; Jain, A. Void reduction in fused filament fabrication (FFF) through *in situ* nozzle-integrated compression rolling of deposited filaments. *Virtual Phys. Prototyp.*, **2021**, 16(2), 146−159.

100 Nam, R.; Jakubinek, M.; Barnes, M. L.; Naguib, H. E. *In situ* cold plasma-enhanced polymer additive manufacturing. *Prog. Addit. Manuf.*, **2026**, 11(4), 3113−3124.

101 Sabyrov, N.; Abilgaziyev, A.; Ali, M. H. Enhancing interlayer bonding strength of FDM 3D printing technology by diode laser-assisted system. *Int. J. Adv. Manuf. Technol.*, **2020**, 108(1), 603−611.

102 Lee, J. E.; Park, S. J.; Son, Y.; Park, K.; Park, S. H. Mechanical reinforcement of additive-manufactured constructs using *in situ* auxiliary heating process. *Addit. Manuf.*, **2021**, 43, 101995.

103 Prajapati, H.; Salvi, S. S.; Ravoori, D.; Qasaimeh, M.; Adnan, A.; Jain, A. Improved print quality in fused filament fabrication through localized dispensing of hot air around the deposited filament. *Addit. Manuf.*, **2021**, 40, 101917.

104 Patel, P.; Rane, R.; Mrinal, M.; Ganesan, V.; Taylor, R.; Jain, A. Characterization of the effect of in-process annealing using a novel print head assembly on the ultimate tensile strength & toughness of Fused Filament Fabrication (FFF) parts. *Virtual Phys. Prototyp.*, **2022**, 17(4), 989−1005.

105 Ravi, A. K.; Deshpande, A.; Hsu, K. H. An in-process laser localized pre-deposition heating approach to inter-layer bond strengthening in extrusion based polymer additive manufacturing. *J. Manuf. Process.*, **2016**, 24, 179−185.

106 Sweeney, C. B.; Lackey, B. A.; Pospisil, M. J.; Achee, T. C.; Hicks, V. K.; Moran, A. G.; Teipel, B. R.; Saed, M. A.; Green, M. J. Welding of 3D-printed carbon nanotube-polymer composites by locally induced microwave heating. *Sci. Adv.*, **2017**, 3(6), e1700262.

107 Kumar, S.; Yoo, D. H.; Song, J. S.; Kim, H. S. Effect of geometric configurations and heat treatment on the tensile properties, joint performance, and failure behavior of 3D-printed carbon and glass fiber composites. *Compos. Part B Eng.*, **2025**, 304, 112693.

聚乳酸(PLA)在熔融沉积成型(FDM)打印中表现出良好的挤出流动性、较高的尺寸稳定性和一定的层间结合能力.然而，PLA层间结合质量远低于材料本体，导致其3D打印件呈现力学各向异性，需从材料、打印工艺和后处理等方面着手调控层间界面结构与性能.

